PAPER NO.
963

STUDY OF CYCLIC PLASTIC STRESSES AT A NOTCH ROOT

By J. H. Crews, Jr., and H. F. Hardrath

Langley Research Center
Langley Station, Hampton, Va.

Presented at

SESA SPRING MEETING

Denver, Colorado

May 5-7, 1965

SOCIETY FOR
EXPERIMENTAL STRESS ANALYSIS
21 BRIDGE SQUARE WESTPORT, CONNECTICUT

A STUDY OF CYCLIC PLASTIC STRESSES AT A NOTCH ROOT

By John H. Crews, Jr., and Herbert F. Hardrath

NASA Langley Research Center
Langley Station, Hampton, Va.

Presented at the Society for Experimental
Stress Analysis Meeting

Denver, Colorado
May 5-7, 1965

A STUDY OF CYCLIC PLASTIC STRESSES AT A NOTCH ROOT

By John H. Crews, Jr., and Herbert F. Hardrath

NASA Langley Research Center

Langley Station, Hampton, Va.

ABSTRACT

13408

An experimental study is presented for cyclic plastic stresses at notch roots in specimens under constant-amplitude repeated tension and reversed loading. Edge-notched, K_T = 2, 2024-T3 aluminum-alloy sheet specimens were cycled until local stress conditions stabilized. Local stress histories were determined by recording local strain histories during cycling and reproducing these histories in simple unnotched specimens. The fatigue lives for these notched specimens were estimated using stabilized local stresses and an alternating versus mean stress diagram for unnotched specimens of the same material. These predictions compared favorably with lives from S-N data for the notch configuration tested.

In addition, an expression is presented for calculating local first-cycle plastic stresses. An acceptable correlation is shown between predicted stresses and experimental data within the scope of the investigation. Authors

LIST OF SYMBOLS

E_s secant modulus corresponding to the local stress at the notch root for monotonically increasing tensile loads, psi

E_s' secant modulus corresponding to the local stress at the notch root for negative loading from tension, psi

E_s'' secant modulus corresponding to the local stress at the notch root for positive loading from compression, psi

E_∞ secant modulus corresponding to the average stress on the net section, psi

K_p plastic stress concentration factor for monotonically increasing tensile loads

K_p' plastic stress concentration factor for negative loading from tension

K_p'' plastic stress concentration factor for positive loading from compression

K_T elastic stress concentration factor

N number of cycles

R ratio of $\frac{S_{min}}{S_{max}}$

S nominal net-section stress, ksi

S_{max} maximum nominal net-section stress, ksi

S_{min} minimum nominal net-section stress, ksi

ΔS nominal stress range, ksi

t specimen thickness, in.

ϵ local strain at the notch root

ρ notch root radius, in.

σ local stress at the notch root, ksi

σ_r local residual stress at the notch root, ksi

INTRODUCTION

Characteristically, fatigue failures in service initiate at geometric discontinuities that produce local stresses higher than the nominal stresses applied. In weight-critical applications these local stresses are frequently in the plastic range. Cyclic loading accompanied by residual stresses, work hardening, and other phenomena leads to fatigue fractures. A basic understanding of the way in which the local stresses are influenced by plastic action should lead to the development of methods for estimating fatigue behavior under constant- and variable-amplitude loading.

The task of analyzing local cyclic stresses is very complex because of the history dependence of the plastic behavior. Thus, the problem has received little attention in the literature.

The present investigation was undertaken as a starting point for relating the local plastic stresses to nominal loading. The local plastic conditions in notched specimens were studied experimentally under constant-amplitude loading. A single material and one specimen configuration were investigated. Preliminary methods for estimating local stresses and fatigue lives were developed. Further study is expected to lead to the development of such methods to include other specimen shapes and materials and for variable-amplitude loading.

EXPERIMENTAL PROCEDURE

Local strain histories at the notch roots of large sheet specimens subjected to cyclic loadings were measured. These strain histories were reproduced in companion unnotched specimens to determine the corresponding stress histories. The stresses and strains obtained in the companion specimen are

expected to represent those of the notched specimen since, in the region of interest, both are subjected to uniaxial stress.

The edge-notched specimen and tensile coupon configurations are shown in figure 1. Dimensions were selected for an elastic stress concentration of two[1]* and for a small ratio of gage length to notch root radius. Notched specimens and companion coupons were machined from adjacent sheet material to minimize variations in material characteristics. In addition, specimen notches were carefully prepared to minimize machining stresses.

Both photoelastic coatings and resistance strain gages were used for strain measurements during the test program. The birefringent coating was bonded to the flat surface of the specimen near the notch and fringe orders at the edge of the notch root were observed with a small-field reflective polariscope. The history of fringe orders was then reproduced in unnotched specimens clad with the same birefringent material. This method required extremely tedious observations and was subject to errors due to edge effects and fringe fadeout at high strain levels. Foil strain gages, bonded in the notch root, proved to be more convenient and reliable and were used for most tests. A small gage length (1/16 inch) was selected to reduce the effects of the strain gradient within the gage length. The load cycling was continued until maximum and minimum local stresses stabilized.

Tests were conducted under repeated tension (R = 0) and completely reversed (R = -1) constant-amplitude loading. Nominal stresses were used over the range from that corresponding to incipient local yielding to that approaching the yield stress of the material on the net section. Guide plates were used to prevent buckling during compressive loadings for both specimens and coupons.

*Numbers refer to references at end of paper.

RESULTS AND DISCUSSION

General

For this study, stress concentration factor is defined as the ratio of local stress at the notch root to the average stress on the net section. Experimental elastic stress concentration factors have been obtained from tensile loading data prior to local yielding. In each test an averaged value for five successively increasing levels of nominal load is calculated, tables 1 and 2. These experimental values have been found to exceed the value of 2.0 from Neuber[1] theory by approximately 5 percent. This discrepancy may be due to the fact that a parallel-sided edge notch is somewhat "sharper" than the Neuber hyperbolic notch for a given notch depth and root radius.

In this paper only stresses at the notch base are studied, and all references to local stress conditions are confined to behavior at this point. The general behavior at this critical point is illustrated in figure 2 for cyclic loading. For the first cycle of repeated loading (R = 0), a typical local behavior is described by the curve OAB; where A represents the maximum local stress and strain and B represents the compressive residual stress and strain occurring upon unloading. For the first cycle of completely reversed loading (R = -1) a typical set of local conditions is described by OABCD where C represents the minimum local stress and strain and D represents the tensile residual stress and strain at the end of the full cycle. The secant moduli shown will be explained later.

Results of this study are summarized in tables 1 and 2 and are discussed in the following sections. In addition, the tables include identification of the strain measuring technique employed for each test. The results appear not

to have been affected significantly by the technique used. Unfortunately, early failures of strain gages were encountered in several tests in which large strain excursions were involved; for these few tests only first-cycle behavior is presented. In general, however, cycling was continued for approximately 30 cycles, which was generally found to result in stabilization of local stresses.

Repeated Loading

Figure 3 illustrates local stress-strain data for the first cycle of repeated loading (R = 0). Local behaviors for six values of maximum nominal stress are presented. The unloading part of each load cycle produced a compressive residual stress. For tests with moderate nominal stresses the residual stresses appeared to be elastic. In tests with high nominal stress local yielding occurred upon unloading.

Maximum and residual local stresses measured during each of several cycles of repeated constant-amplitude loading are shown in figure 4. The three pairs of curves represent typical histories of maximum stress and of compressive residual stress for three different levels of nominal stress. A small reduction in maximum local stresses was observed during the first few cycles with a corresponding increase in compressive residual stresses. Thus the mean local stress decreased somewhat while the local stress range remained virtually unchanged during these cycles. Beyond the tenth cycle, local stresses returned to essentially the same values in each cycle. These local stabilized stresses and those presented in table 1 for other tests will be used later in estimating fatigue life for the specimens tested.

Reversed Loading

The local stress-strain histories measured during the first cycle in each of several tests with completely reversed loadings are presented in figure 5. For these tests four characteristic values of local stress are of interest: the maximum, residual after unloading (half-cycle), the minimum, and the residual after completing the cycle (full-cycle). The loci of the residual stresses as influenced by the nominal stress are also shown in the figure. As was the case with tests at $R = 0$, the residual stresses are subject to some plastic action for tests in which high nominal stresses were applied. The half-cycle and full-cycle values of residual stress for a given load level were approximately symmetrical about zero except for the test of $S = 25$ ksi. This dissymmetry is attributable to the fact that more plastic action occurred in compression than in tension.

Typical histories of these four characteristic stresses during subsequent cycles of reversed loading are presented in figure 6. The absolute values of maximum and minimum stresses increased appreciably thus increasing the local stress range during each of the first 15 to 20 cycles, after which the stress range remained stable. Similarly, the absolute values of residual stress decreased during each of these cycles and then stabilized. The stabilized values of maximum and minimum stresses were approximately symmetric about zero.

Fatigue Estimates

The stabilized values of local stress described above were used to estimate the fatigue lives of similar notched specimens tested at the same nominal stress levels. The fatigue data used for the comparisons were for

edge-notched 2024-T3 aluminum-alloy sheet specimens with $K_T = 2$ and subjected to constant-amplitude axial loads with $R = 0$ and $R = -1$.[2,3]

The lives were obtained on the assumption that failure would occur in the notched specimen in the same number of cycles that produced failure in unnotched specimens subjected to the repeated stresses equal to the local stabilized stresses observed in the present tests. The estimates were taken from a diagram of alternating versus mean stresses for tests of unnotched specimens of the same material.[4]

The resulting estimates of life and fatigue data are listed in table 3, and are plotted in figure 7. The estimates agree well with the data except at low nominal stress levels. The lack of agreement at the low levels might be attributed to the fact that a larger number of cycles is required to propagate a crack to critical size at low stress levels than at higher levels. Obviously, this part of fatigue behavior is not represented adequately by the assumptions used for the present estimates. At higher stress levels somewhat less propagation takes place, and only small errors are introduced by ignoring this mechanism beyond that part which is also present in the fatigue failure of unnotched specimens.

The above trends are encouraging because they offer the hope that fatigue lives of notched parts can be estimated from behavior of unnotched specimens provided that the effects of notches and plastic action can be accounted for. Unfortunately, the key information needed to accomplish the estimate is the relation between the applied nominal stresses and the stabilized local stresses. To this point, this relationship is obtainable only by rather painstaking tests. The following section presents some preliminary thoughts on a method for computing the desired local stresses for the first cycle of loading.

LOCAL STRESS CALCULATIONS

Proposed Method

Previous studies of stress concentration factors as modified by plastic action have been conducted at the NASA Langley Research Center.[5,6] Briefly, these studies have led to the development of the following generalized formula:

$$\sigma = SK_p = S\left[1 + (K_T - 1)\frac{E_S}{E_\infty}\right] \tag{1}$$

This relation yields, within engineering accuracy, estimates of local plastic stresses for arbitrary stress raisers under monotonically increasing loads, at least for small plastic strains (up to 1 or 2 percent). The stress A in figure 2 is determined by a trial-and-error solution of equation (1).

For unloading from point A an additional term must be added to the above equation. The basic approach in developing this term can be easily understood if unloading from point A is considered to be a negative application of nominal loading. From this viewpoint, it follows that the local stress for any level of negative load might be found by the use of an appropriate stress concentration factor. This approach will be used in the following: Attention will be restricted first to residual stresses and then generalized to include the entire range AC.

In cases where no plastic yielding occurs during the negative loading the desired stress concentration factor is K_T. For an unloaded specimen the residual stress F in figure 2 is calculated from the equation

$$\left.\begin{aligned}\sigma_r &= \sigma_{max} - S_{max}K_T \\ \sigma_r &= S_{max}(K_p - K_T)\end{aligned}\right\} \qquad (2)$$

However, if local compressive yielding occurs, K_T no longer applies and a plasticity correction is required. It is proposed that this plasticity correction may be obtained by a method involving secant moduli similar to that employed for equation (1). A typical secant modulus E_s' required for this calculation is shown in figure 2. It has its origin at point A, the point at which unloading began. The following relation is proposed for calculating compressive residual stresses in the plastic range:

$$\sigma_r = S_{max}(K_p - K_p') \qquad (3)$$

where K_p' = plastic stress concentration for negative loading (unloading)

$$K_p' = 1 + (K_T - 1)\frac{E_s'}{E_\infty}$$

The range of applicability of equation (3) may be readily extended to solve the general case of any negative loading from tension that results in compressive yielding:

$$\sigma = S_{max}K_p - (S_{max} - S)K_p' \qquad (4)$$

where S is the nominal stress for which σ is sought.

This relation is a generalization of the three preceding expressions and is applicable for the full range of local stress represented by OABC in figure 2.

If the procedure of unloading from point A to establish E_s' values is repeated for positive loading from point C in figure 2, the appropriate secant

modulus E_s'', may also be found in order to calculate the local stress for any level of load. The addition of another term to equation (4) leads to an expression for the local behavior during the fourth quarter cycle of loading:

$$\sigma = S_{max}K_p - (S_{max} - S_{min})K_p' - (S_{min} - S)K_p'' \qquad (5)$$

K_p'' = plastic stress concentration factor for the third excursion into the plastic range

$$K_p'' = 1 + (K_T - 1)\frac{E_s''}{E_\infty}$$

where E_s'' is the appropriate secant modulus referenced to the minimum local stress (C in fig. 2) experienced.

These equations require trial-and-error solution similar to that used to solve equation (1). In principle, the stress-strain curves AC and CD are required for the particular previous stress history experienced during prior load excursions.

Comparison With Data

For each level of nominal stress, a simple unnotched specimen was loaded in a manner such that the notch strain history was reproduced, as previously explained. Therefore, for each test a stress-strain curve similar to that of figure 2 was obtained for the first cycle. The segments of each curve corresponding to OA were found to be generally similar and a faired stress-strain curve was used in establishing values of E_s. In addition, the segments corresponding to AC for each test were also found to have essentially equal elastic ranges and consistent shapes for the early stages of the plastic

range. Therefore, a single faired curve was also used to determine values of E_s'. The curves of K_p and K_p' shown in figure 8 were calculated for the full range of loads with the aid of these faired stress-strain curves.

The similar shapes of the local stress-strain curves for unloading from A and unloading from C suggest another simplifying assumption. The assumption made is that the segment CD, of the stress-strain curve in figure 2, has the same shape as the segment AB. Thus, the single curve for K_p' in figure 8 may be used to compute the K_p'' in equation (5). However, K_p' and K_p'' must be evaluated independently for the particular nominal stress range over which each acts. These separate evaluations preclude the combination of K_p' and K_p'' terms in equation (5).

Equation (4) was used with the curves of K_p and K_p' to calculate first-cycle local stresses for repeated (R = 0) loading. The maximum local stresses were calculated by setting $S = S_{max}$ in this equation, thus reducing it to equation (1). The compressive residual stresses at the end of the first full cycle were found by setting $S = 0$. With this substitution the generalized equation reduces to equation (3). These calculated stresses are compared in figure 9 with the first-cycle test data in the range investigated. For a point-by-point comparison, data and calculated results are also presented in table 1.

An acceptable correlation is observed. The minor discrepancies at high load levels are probably attributable to the use of the photoelastic coating technique in these tests, while the faired stress-strain curves were based entirely on data obtained by strain-gage instrumentation.

For reversed loading (R = -1) equations (4) and (5) were used to calculate local stresses. Maximum local and compressive residual stresses were calculated

as in the above case of repeated loading from equation (4). Equation (4) was also used to calculate minimum local stresses by setting $S = S_{min}$. Equation (5) and the curve of K_p' in figure 8 were used to calculate tensile residual stresses occurring at the end of a first-cycle of completely reversed loading. These four characteristic stresses and the corresponding observed data are listed in table 2 and are shown in figure 10.

With the exception of tensile (full-cycle) residual stresses, good correlation is illustrated by figure 10 between calculated curves and test data. The assumption regarding the similarity in stress-strain curves for unloading from both tension and compression is possibly responsible for the errors in predicted full-cycle stresses. The occurrence of full-cycle residual stresses at nominal stresses lower than required to produce half-cycle residual stresses is clearly illustrated in this figure.

Deviations of individual stress-strain curves from the faired curves used in calculating K_p and K_p' are expected to account for some discrepancies in all calculated stresses. Calculations and data based entirely on the behaviors of a given specimen and its companion simple specimen were found to be in excellent agreement.

In general, an acceptable correlation is displayed between the calculated results and the experimental data found in this study. A continued evaluation of the proposed equations should prove them applicable for other arbitrary stress raisers during the first load cycle.

As demonstrated in this paper, estimates of stabilized stresses would be useful in predicting fatigue of notched components. The equations presented herein, if found to hold for arbitrary geometries and other materials in the first cycle of loading, will serve as an important step in calculating these

stabilized conditions at a stress raiser. Further, the information regarding residual stresses obtained in this study should be useful for explaining the nonlinear accumulation of damage observed in variable-amplitude fatigue tests.

CONCLUSIONS

From this study of plastic stress histories at a notch root under constant-amplitude load cycling, the following conclusions are made:

1. Stabilization of local stresses occurred in less than 30 cycles for the edge-notched specimens of sheet 2024-T3 aluminum alloy employed in this study.

2. Within the range of nominal stresses used in this investigation, only small variations were observed in local plastic stresses for repeated ($R = 0$) loading. A small reduction in maximum local stresses was observed during the first few cycles with a corresponding increase in compressive residual stresses. Thus the mean local stress decreased somewhat while the local stress range remained virtually unchanged during these cycles.

3. Completely reversed ($R = -1$) load cycling resulted in noticeable increases in both maximum and minimum local stresses before stabilization occurred. Compressive residual stresses measured at the end of each half-cycle and tensile residual stresses measured at the end of each full cycle decreased significantly before stabilizing.

4. Useful fatigue predictions were made for the notched specimens from stabilized local stress conditions and an alternating versus mean stress diagram for unnotched specimens of the same material.

5. The generalized notch stress equation, presented in this paper, adequately described local plastic stress behavior for the first cycle of loading within the range of this investigation.

REFERENCES

1. H. Neuber, Theory of Notch Stresses, Principles for Exact Calculation of Strength With Reference to Structural Form and Material, J. W. Edwards (Ann Arbor, Mich.), 1946.
2. W. Illg, Fatigue Tests on Notched and Unnotched Sheet Specimens of 2024-T3 and 7075-T6 Aluminum Alloys and of SAE 4130 Steel With Special Consideration of the Life Range From 2 to 10,000 Cycles, NACA TN 3866, 1956.
3. H. J. Grover, S. M. Bishop, and L. R. Jackson, Fatigue Strengths of Aircraft Materials. Axial-Load Fatigue Tests on Notched Sheet Specimens of 24S-T3 and 75S-T6 Aluminum Alloys and of SAE 4130 Steel With Stress-Concentration Factors of 2.0 and 4.0, NACA TN 2389, 1951.
4. H. J. Grover, W. S. Hyler, P. Kuhn, C. B. Landers, and F. M. Howell, Axial-Load Fatigue Properties of 24S-T and 75S-T Aluminum Alloy as Determined in Several Laboratories, NACA Report 1190, 1954.
5. E. Z. Stowell, Stress and Strain Concentration at a Circular Hole in an Infinite Plate, NACA TN 2073, 1950.
6. H. F. Hardrath, and L. Ohman, A Study of Elastic and Plastic Stress Concentration Factors Due to Notches and Fillets in Flat Plates, NACA Report 1117, 1953.

TABLE 1.- LOCAL STRESS DATA AND CALCULATED RESULTS

FOR REPEATED LOADING (R = 0)

S_{max}, ksi	Exp'l method*	$K_{T_{elast}}$, (exp'l)	Maximum local stress, ksi			Residual stress, ksi		
			First cycle		Stabilized	First cycle		Stabilized
			Exp'l	Calc'd		Exp'l	Calc'd	
25	SG	2.13	51.3	51.0	51.1	-1.8	-1.5	-2.0
30	PC	2.14	53.0	52.2	51.0	-11.7	-10.8	-13.0
35	SG	2.15	53.9	53.4	52.5	-19.6	-19.6	-21.7
40	PC	2.04	53.9	55.4	52.8	-27.7	-26.6	-29.8
45	PC	2.09	56.0	57.8	55.0	-35.0	-32.2	-37.0
50	PC	2.09	57.0	60.5	55.5	-40.4	-34.4	-43.0

*SG = Strain gage; PC = Photoelastic coating.

TABLE 2.- LOCAL STRESS DATA AND CALCULATED RESULTS FOR REVERSED LOADING (R = -1)

S_{max}, ksi	Exp'l method*	$K_{T_{elast}}$, (exp'l)	Maximum local stress, ksi			Half-cycle residual stress, ksi			Minimum local stress, ksi			Full-cycle residual stress, ksi		
			First cycle		Stabilized	First cycle		Stabilized	First cycle		Stabilized	First cycle		Stabilized
			Exp'l	Calc'd		Exp'l	Calc'd		Exp'l	Calc'd		Exp'l	Calc'd	
25	SG	2.16	52.4	51.0	53.5	-1.5	-1.5	0	-44.7	-44.5	-45.5	10.2	8.0	9.2
30	SG	2.12	51.4	52.2	56.0	-12.8	-10.8	-7.5	-49.6	-51.0	-54.5	15.5	12.0	10.0
35	SG	2.15	52.9	53.4	61.0	-21.4	-19.6	-12.5	-53.8	-55.4	-59.5	20.9	17.6	15.0
40	SG	2.12	53.6	55.4		-27.3	-26.6		-55.9	-59.0		27.1	23.0	
45	SG	2.13	56.5	57.8		-32.9	-32.2		-62.9	-63.7		32.7	26.3	
50	SG	2.10	58.2	60.5		-37.9	-34.4		-67.2	-67.8		36.3	27.5	

*SG = Strain gage.

TABLE 3.- ESTIMATES OF FATIGUE LIFE

[K_T = 2, 2024-T3 aluminum alloy]

S_{max}, ksi	R	Observed life, cycles (a)	Estimated life, cycles
25	0	190,000	[b]72,500
30	0	83,000	[b]45,700
35	0	46,000	[b]30,900
40	0	27,500	[b]24,000
45	0	16,500	[b]17,000
50	0	10,500	[b]13,700
25	-1	19,500	[c]10,000
30	-1	7,300	[c]5,000
35	-1	2,750	[c]2,000

[a]Observed lives taken from references 2 and 3.

[b]Estimates based on data for unnotched specimens from reference 4.

[c]Estimates based on data for unnotched specimens from reference 2.

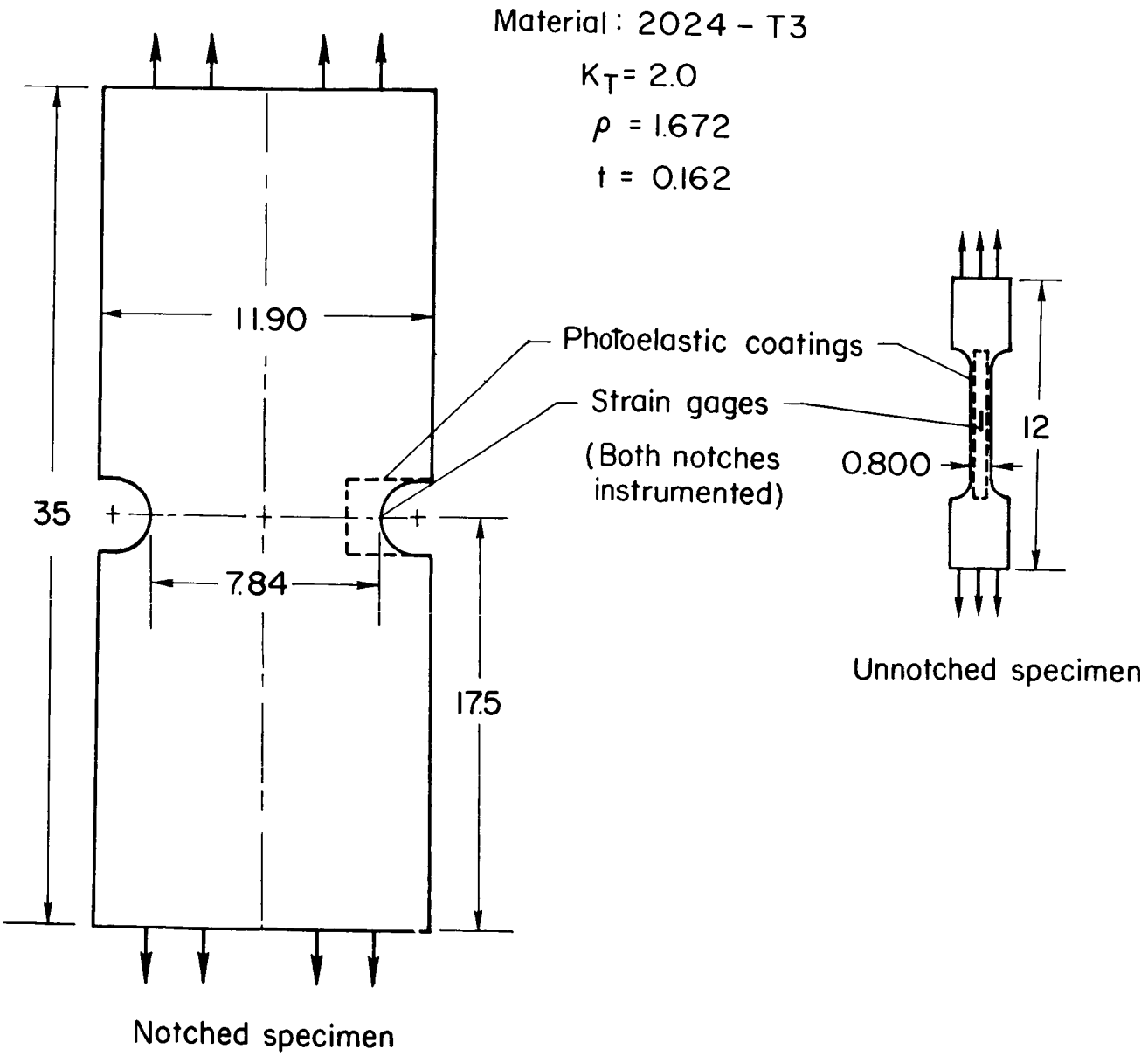

NASA

Figure 1.- Specimen dimensions and instrumentation (all dimensions are in inches).

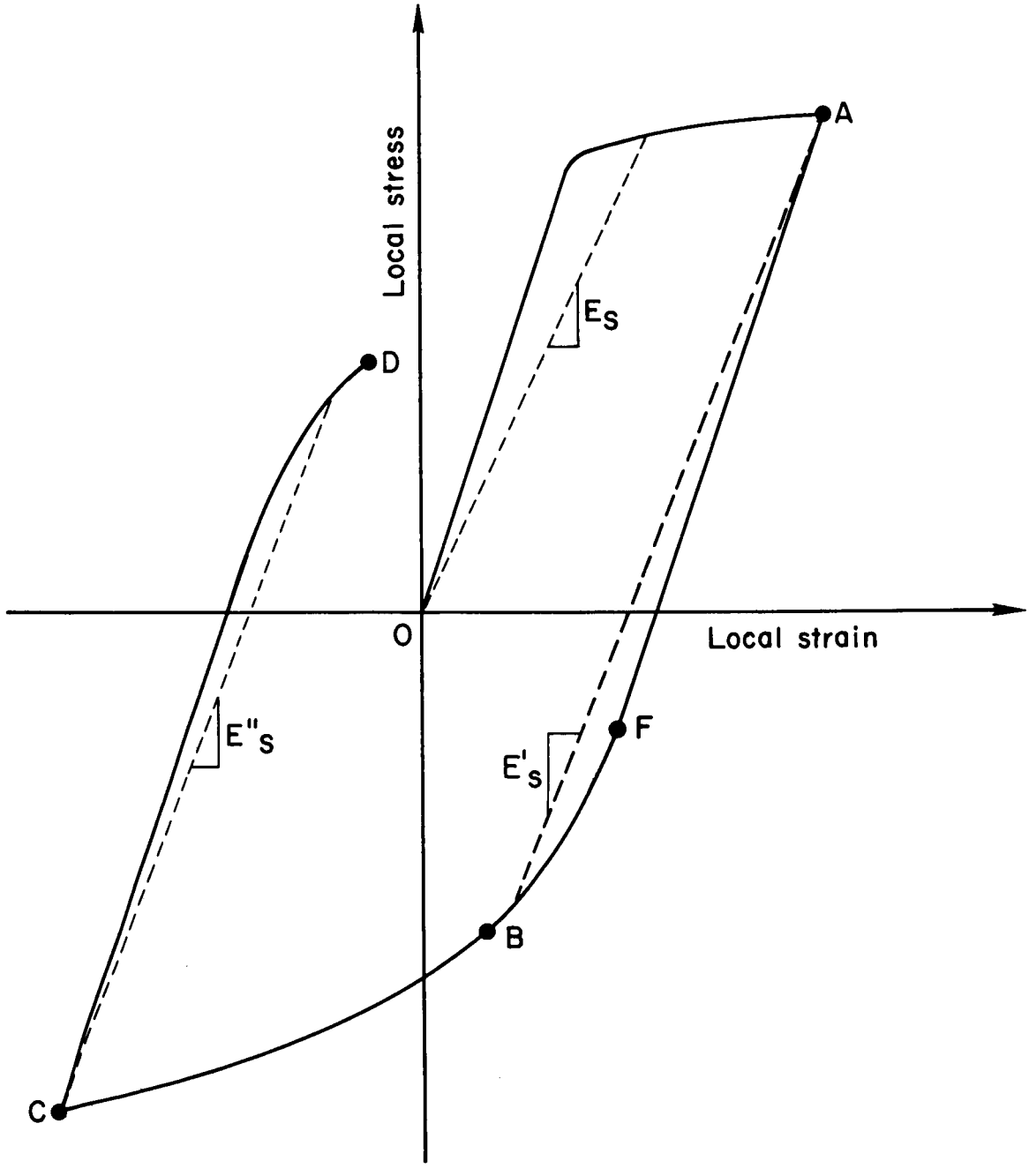

NASA

Figure 2.- Local stress-strain curve for first cycle of loading.

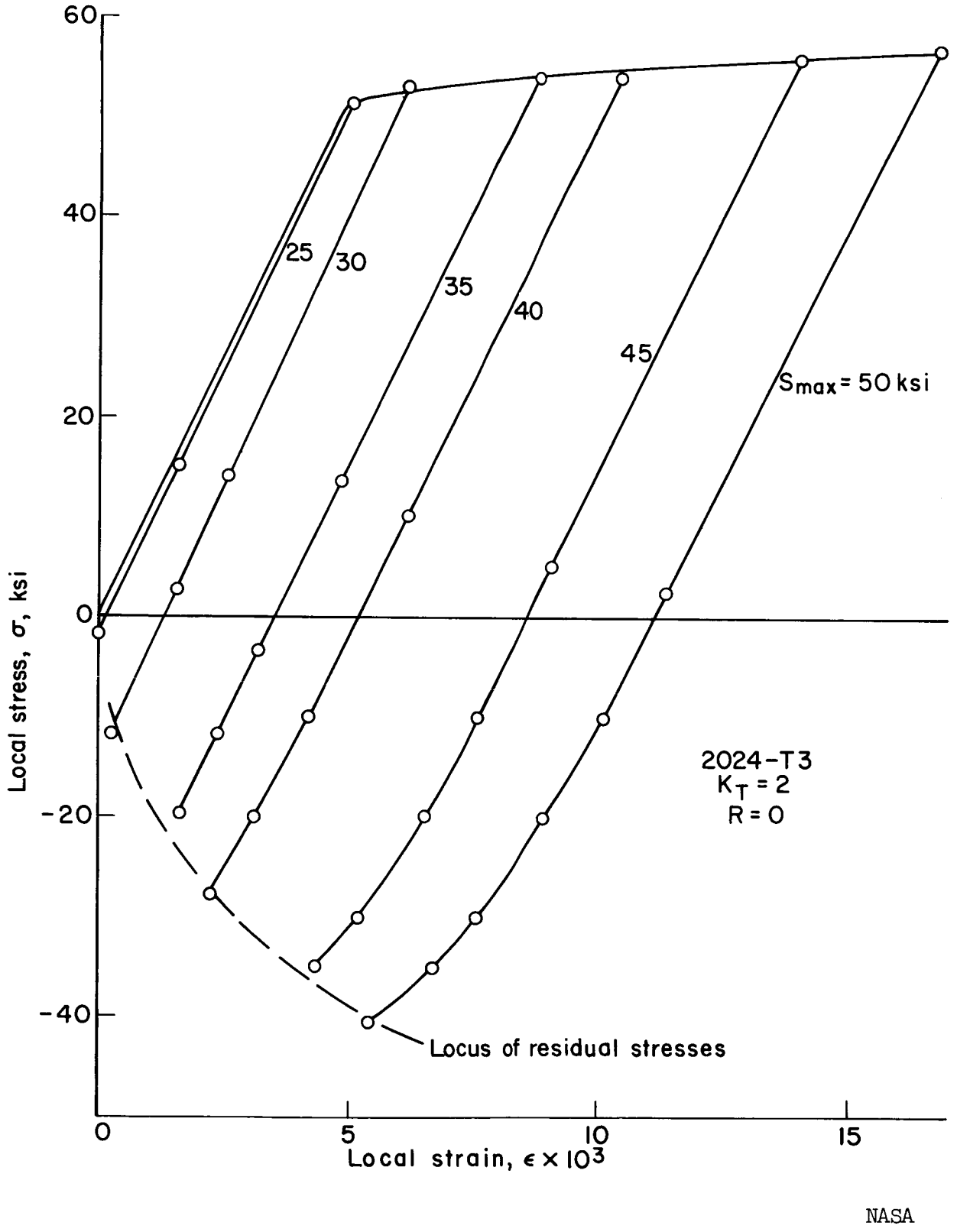

Figure 3.- Local stress-strain curves for first cycle repeated (R = 0) loading.

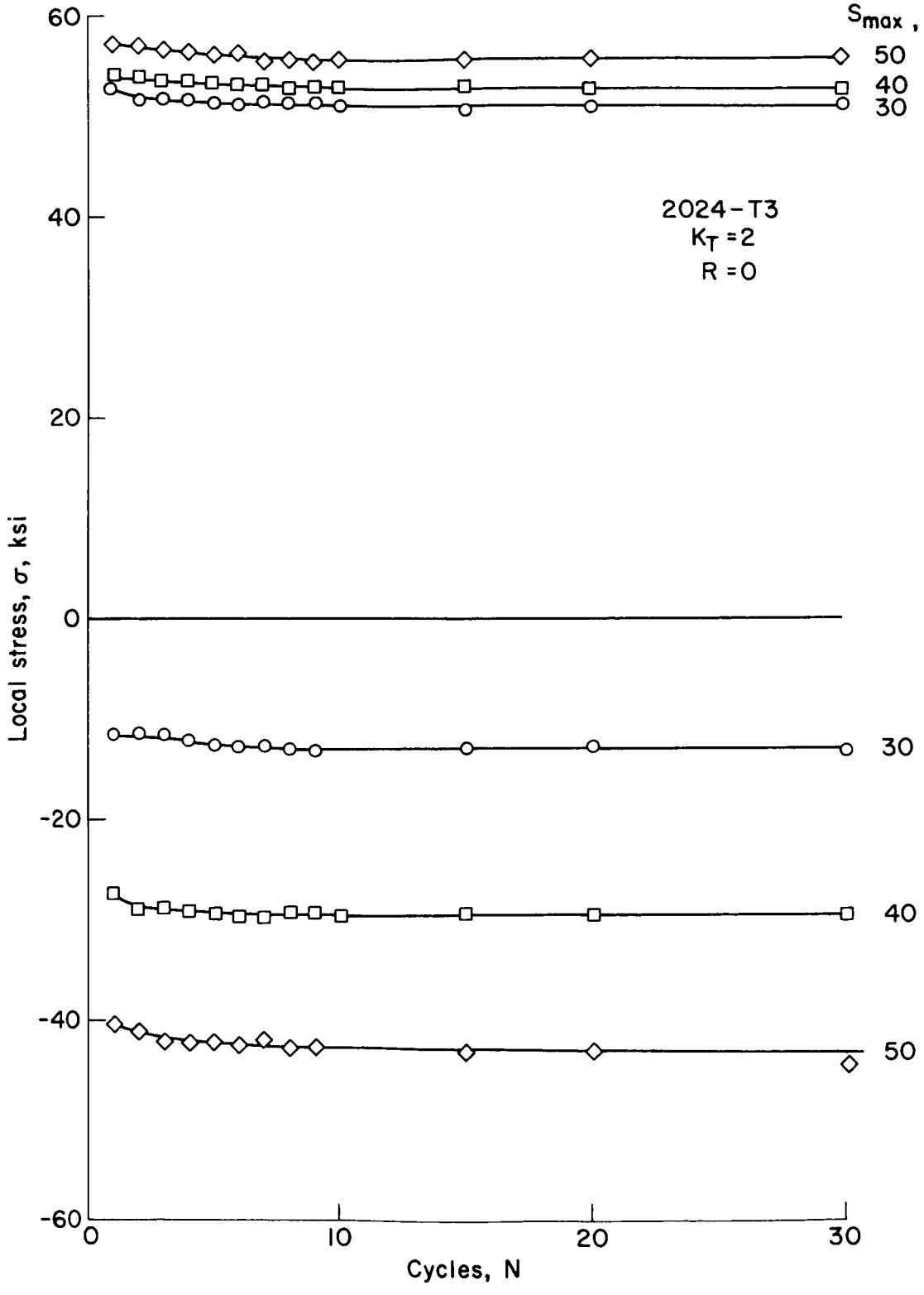

Figure 4.- Stabilization of local stresses for repeated (R = 0) constant-amplitude loading.

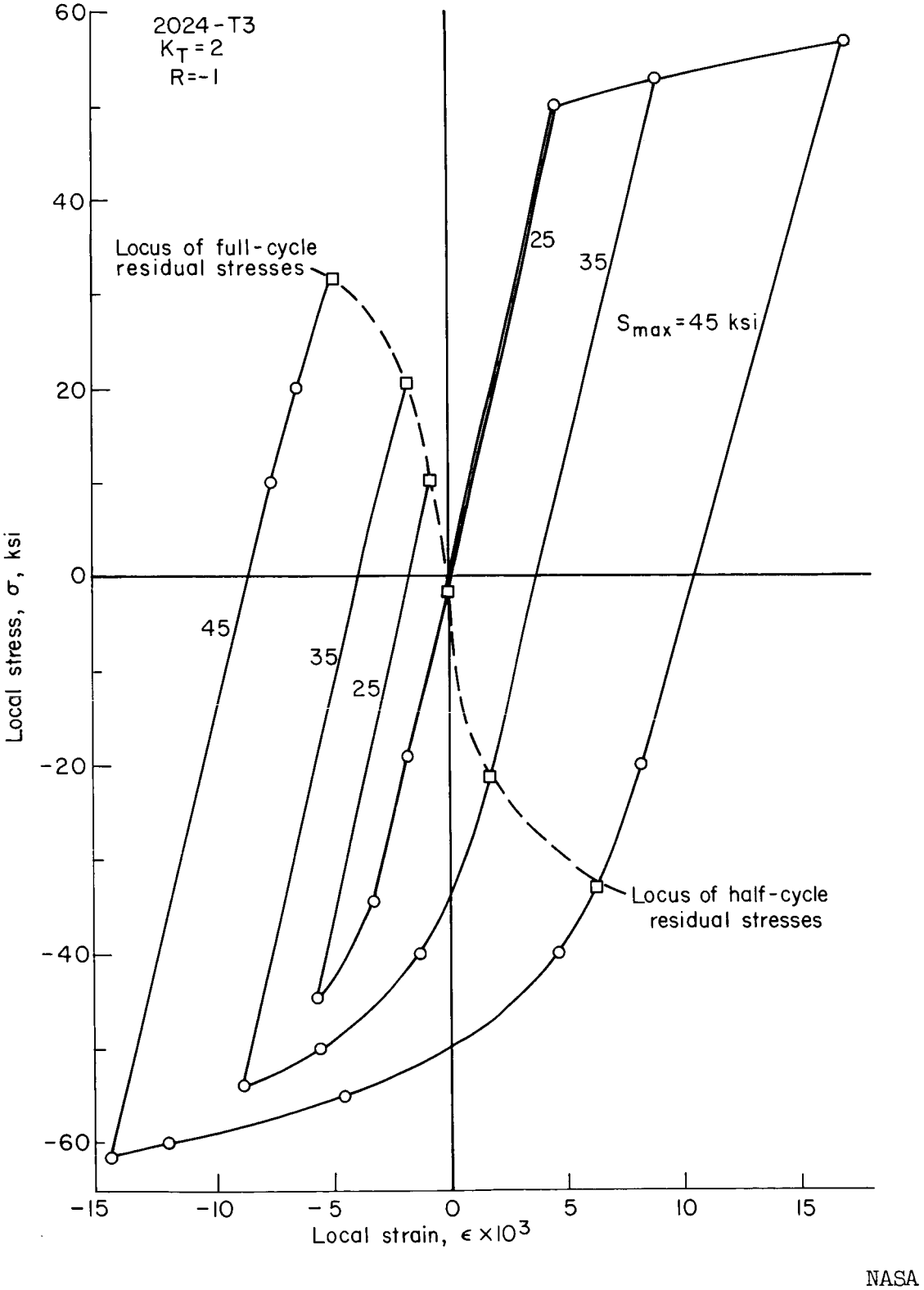

NASA

Figure 5.- Local stress-strain curves for first cycle of reversed (R = -1) loading.

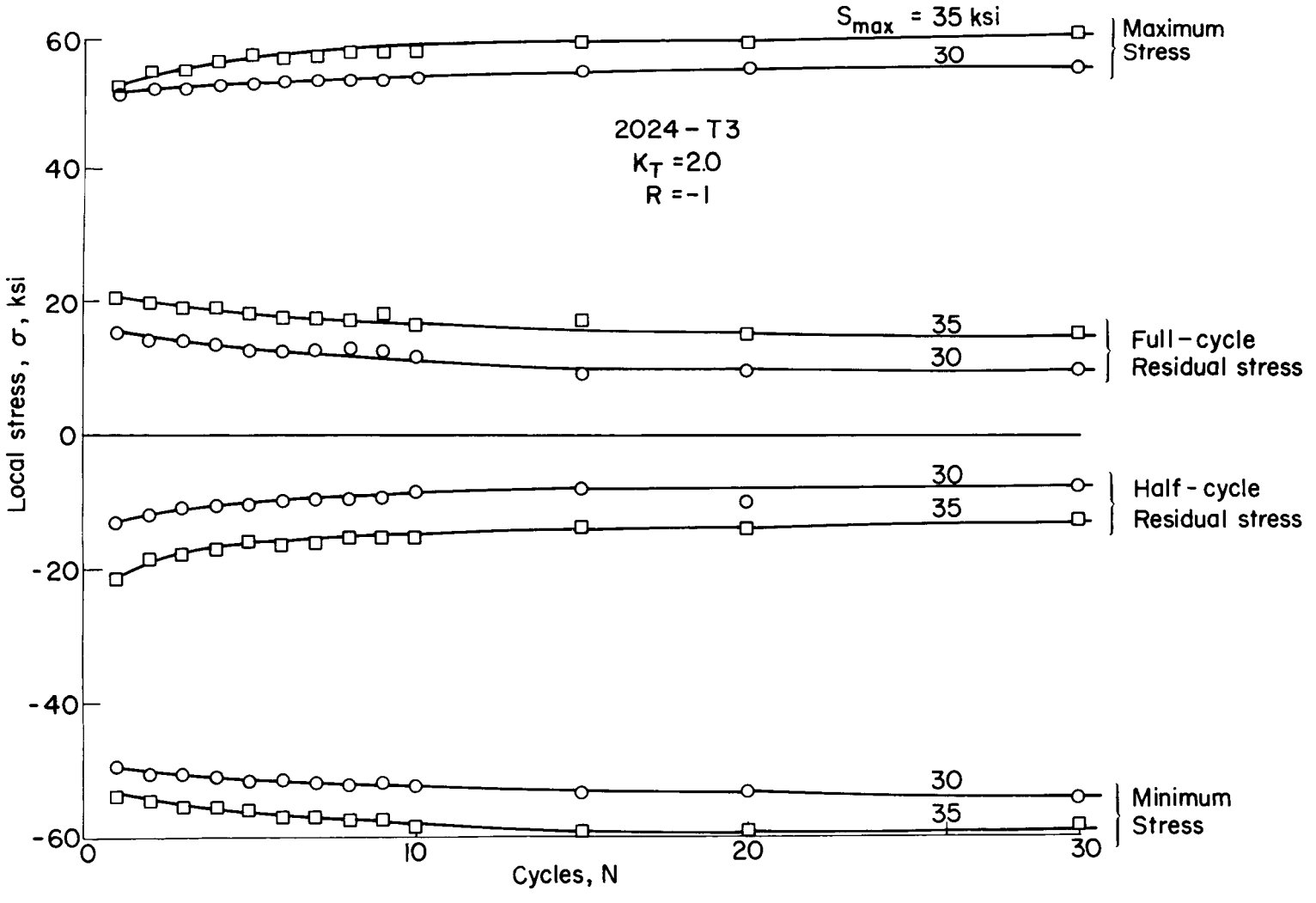

Figure 6.- Local stress stabilization for reversed (R = -1) constant-amplitude loading.

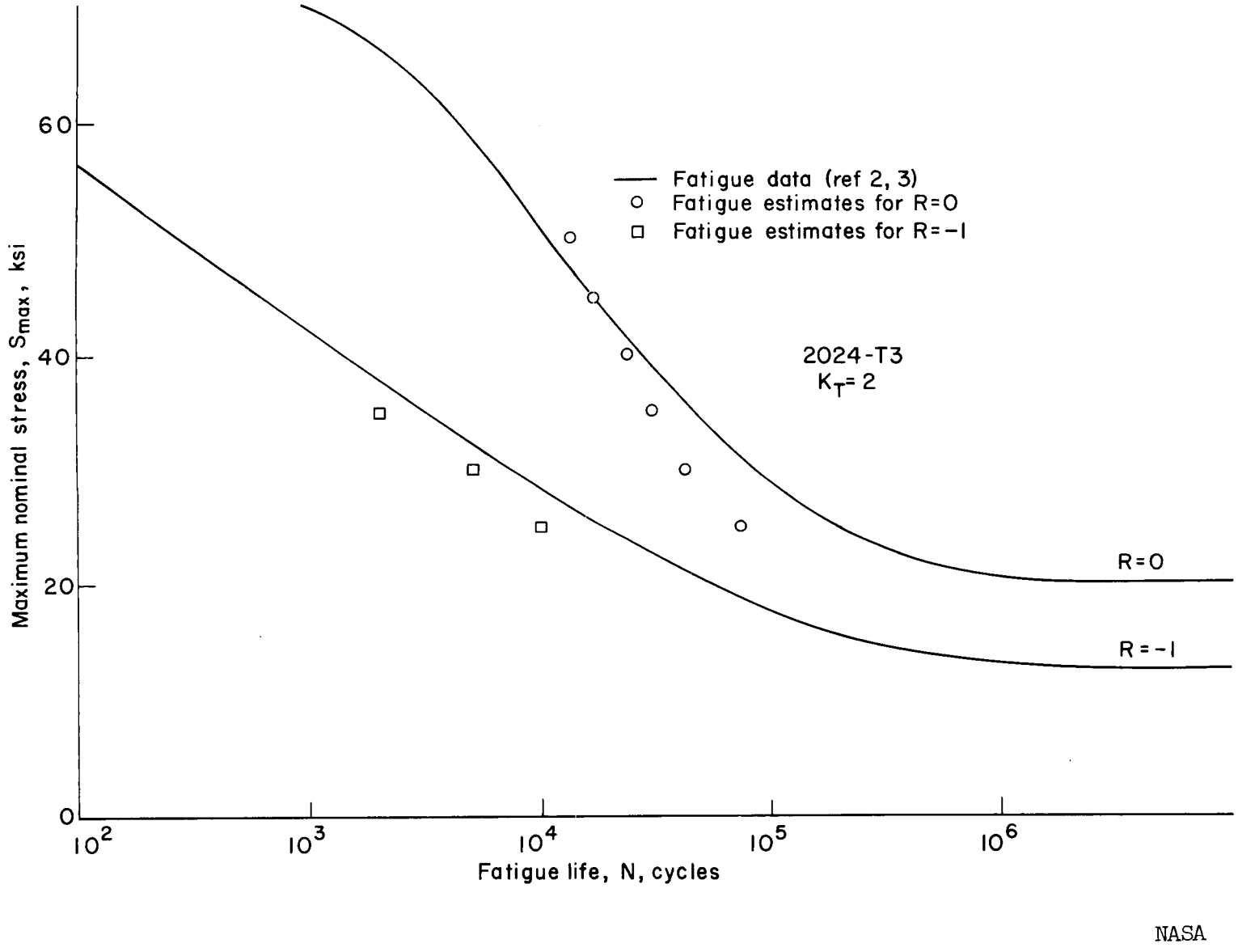

Figure 7.- Fatigue predictions.

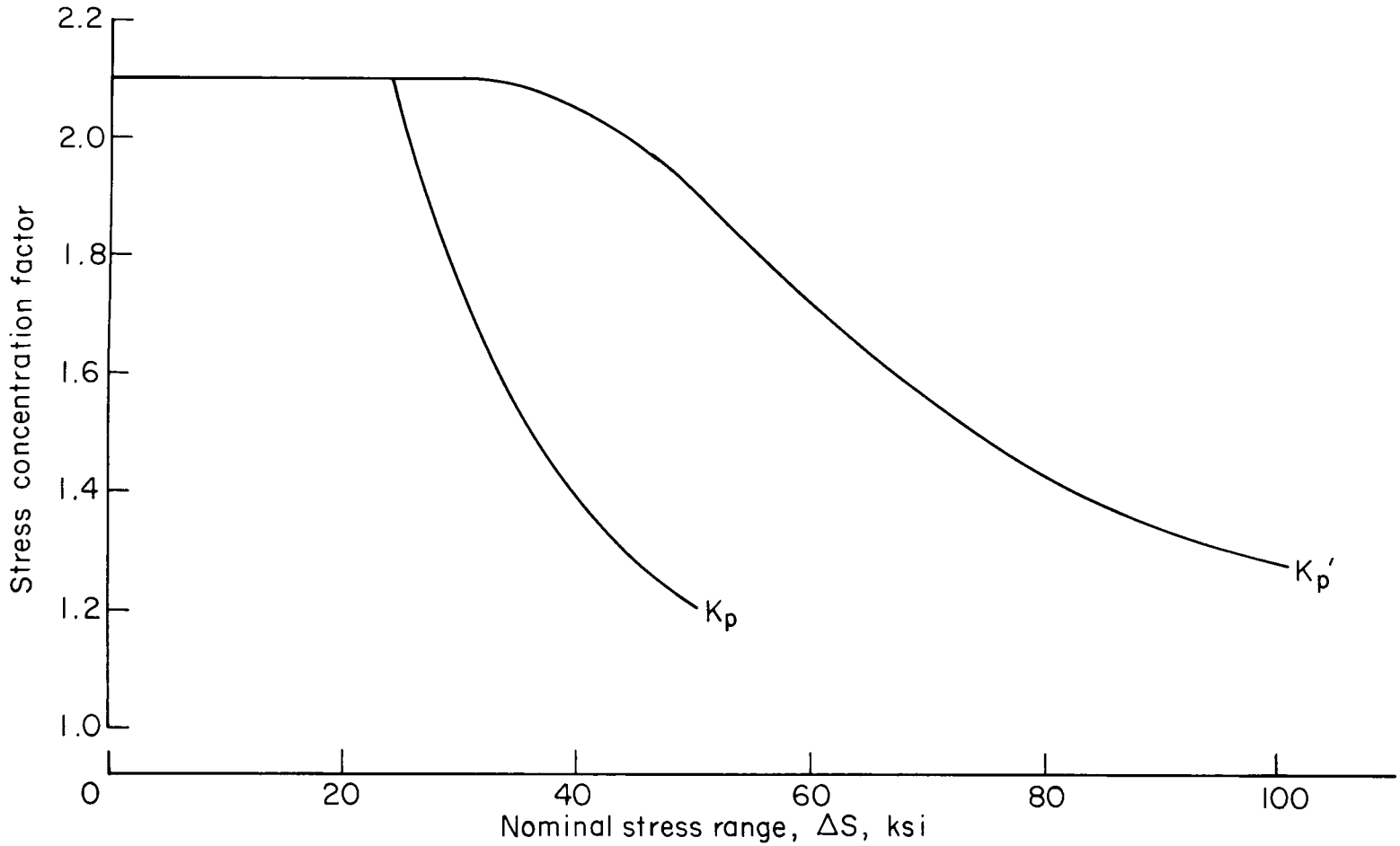

Figure 8.- Plastic stress concentration factors.

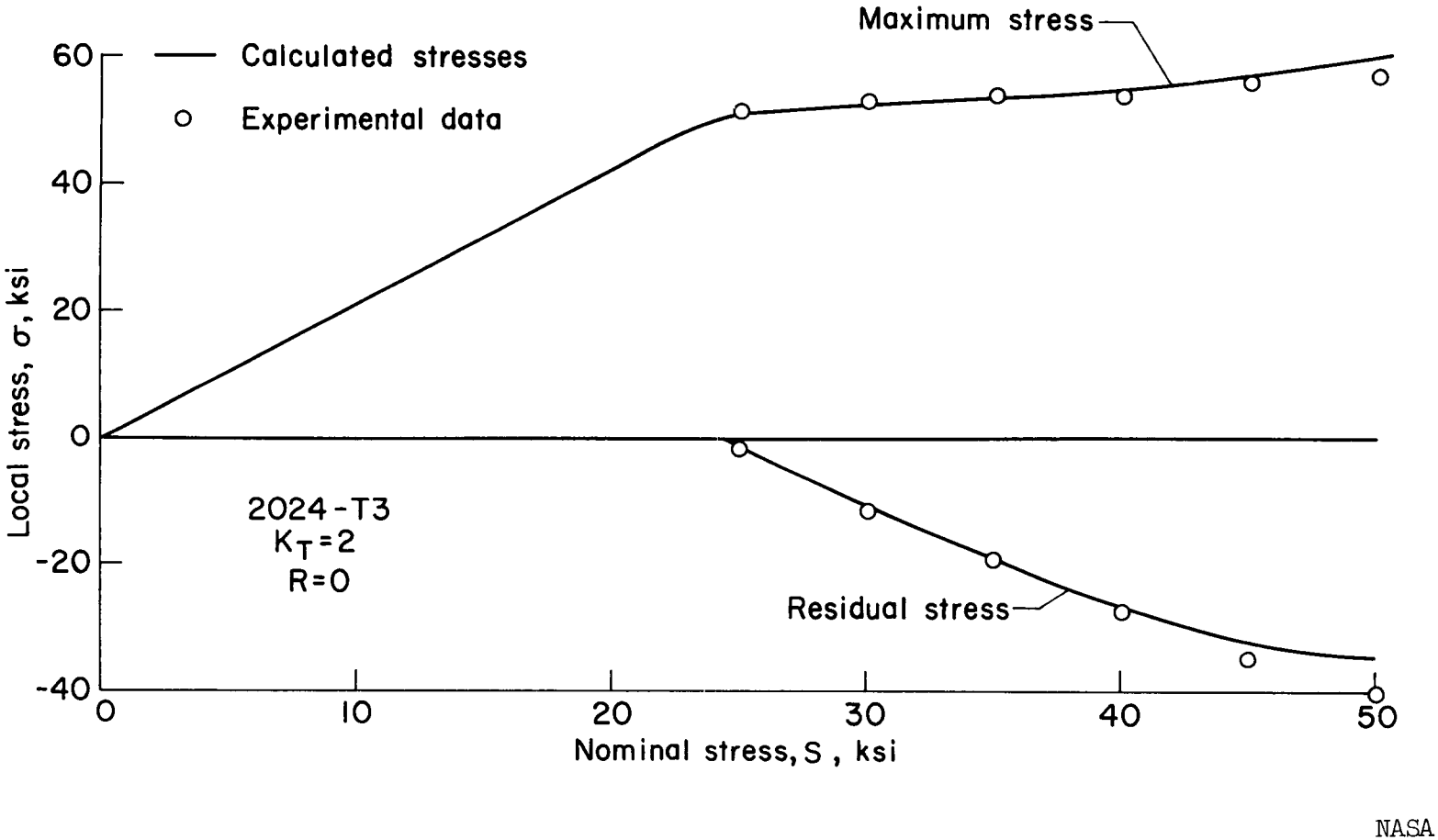

Figure 9.- First-cycle stresses for repeated loading.

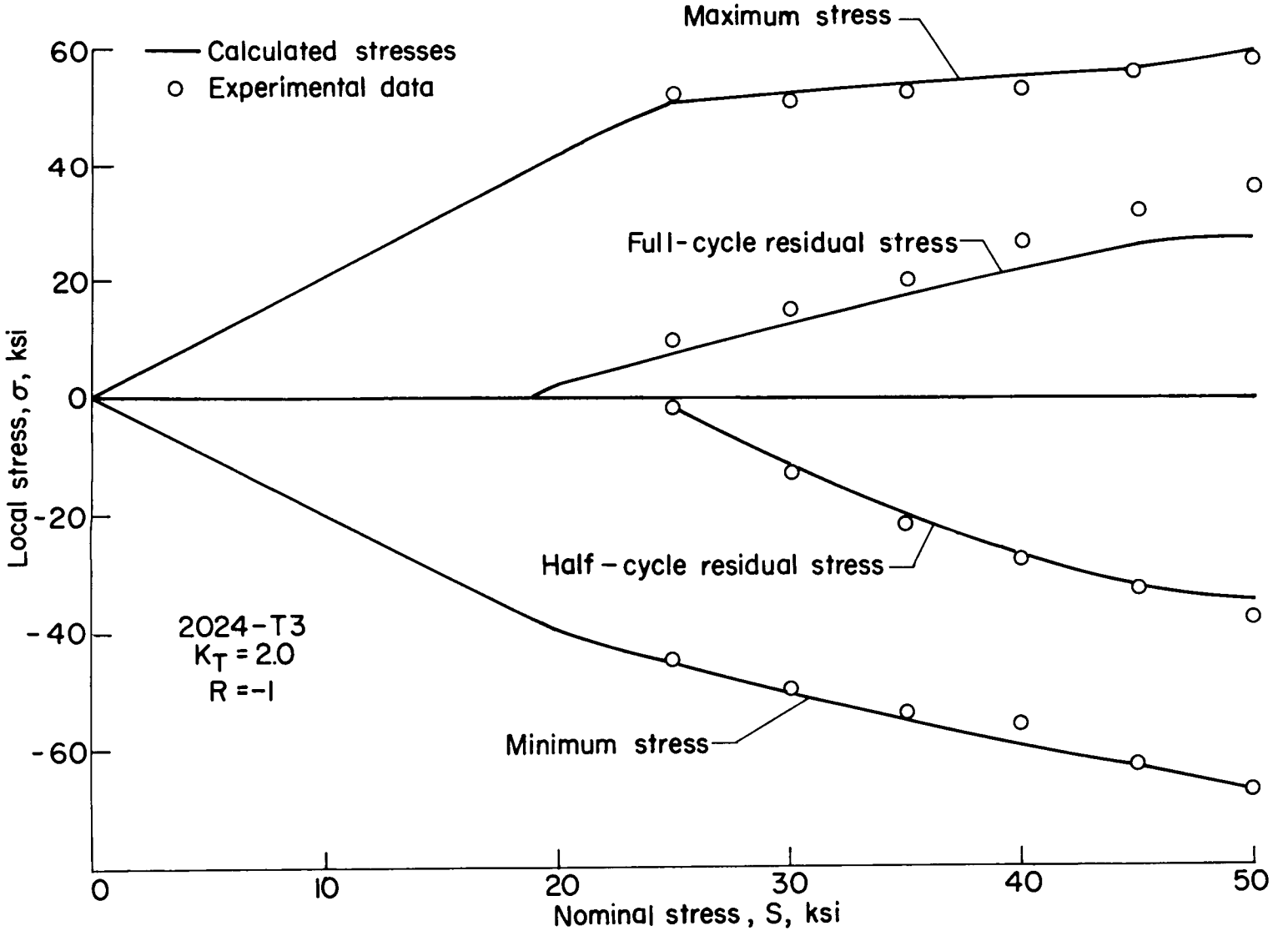

Figure 10.- First-cycle stresses for completely reversed loading.